THE ASTROPHYSICAL JOURNAL, 409:345–359, 1993 May 20

POSTGLITCH RELAXATION OF THE VELA PULSAR AFTER ITS FIRST EIGHT LARGE GLITCHES: A REEVALUATION WITH THE VORTEX CREEP MODEL

M. ALI ALPAR
Physics Department, Middle East Technical University, Ankara 06531, Turkey
H. F. CHAU[1] AND K. S. CHENG
Department of Physics, University of Hong Kong, Pokfulam Road, Hong Kong, Pokfulam Road, Hong Kong
AND
DAVID PINES
Department of Physics, University of Illinois at Urbana-Champaign, Urbana, IL 61801
Received 1992 February 25; accepted 1992 October 7

ABSTRACT

We present a comprehensive reevaluation of eight of the nine glitches observed to date from the Vela pulsar, and the postglitch relaxation following each glitch. All glitch data sets can be described in terms of three distinct components of short and intermediate time scale exponential relaxation, followed by a long-term recovery of the glitch-induced change in the spin-down rate that is linear in t, $\Delta\dot{\Omega}_c(t) \propto t$. We interpret the short and the intermediate time scale exponential relaxation, characterized by relaxation times of 10 hr, $3^d.2$, and 32^d as the linear response of vortex creep in those regions of the pinned superfluid in the neutron star crust through which no sudden vortex motion occurred at the time of the glitch. The long-term recovery is interpreted as the nonlinear response of vortex creep regions. In addition, there are regions of the crustal superfluid which cannot sustain a vortex density or vortex creep current, but which play a significant role in determining the angular momentum balance. The tendency of glitches to leave permanent spin-up remnants is explained as a discrete internal torque which in glitches, couples part of the crustal superfluid to the observed crust. We find that, on average, the theoretically expected interglitch intervals agree quite well with the observed intervals.

The same set of short and intermediate relaxation times, with similar values of moments of inertia for the various components of the crustal superfluid, yield good fits for all postglitch data sets. Furthermore, these relaxation times and moments of inertia are compatible with previous theoretical estimates. A moment of inertia fraction of at least 0.024 is implied for the crustal superfluid. This result rules out neutron star models based on soft equations of state.

Subject headings: dense matter — pulsars: individual (Vela) — stars: neutron

1. INTRODUCTION

Pulsar glitches (sudden frequency jumps of magnitude $[\Delta\Omega/\Omega] \sim 10^{-9}$ to 10^{-6}, accompanied by jumps in the spin-down rate, of magnitude $[\Delta\dot{\Omega}/\dot{\Omega}] \sim 10^{-3}$ to 10^{-2}) are now established as common phenomena, probably experienced by pulsars of all ages, but more frequently in younger pulsars. The Vela pulsar, PSR 0833−45, has been a particularly prolific and interesting source of glitches, having supplied us with nine large glitches with $(\Delta\Omega/\Omega) \sim 10^{-6}$ and $(\Delta\dot{\Omega}/\dot{\Omega}) \sim 10^{-2}$ at intervals of a few years since the glitch observation in 1969 (Radhakrishnan & Manchester 1969; Reichley & Downs 1969) (for data fitting and references for the first six glitches see Cordes, Downs, & Krause-Polstorff 1988; results for glitches seven and eight are reported by Klekociuk et al. 1985a, b and by Hamilton et al. 1989, McCulloch et al. 1990, Flanagan 1989, 1990a, b). The most recent, ninth, glitch (Flanagan 1991) is not included in the present study. The Crab pulsar (Lyne & Pritchard 1987; Lyne 1991) and the recently discovered PSR 1737−30, whose age and glitch activity are comparable to Vela's (McKenna & Lyne 1990) are the two other young pulsars to have experienced frequent glitches. The early glitches of the Vela pulsar were detected typically with an uncertainty of a week or longer in the actual date of the glitch. More recently, a continuous monitoring effort by Australian and South African observers has resulted in uncertainties of less than a week for the fifth glitch, and less than a day for the sixth and seventh glitches (McCulloch et al. 1981, 1983; Hamilton, McCulloch, & Royle 1982; Klekociuk et al. 1985a, b). The eighth glitch actually took place during an observing session (Hamilton et al. 1989; Flanagan 1989). The *immediate* postglitch relaxation has been observed (Flanagan 1990a; McCulloch et al. 1990) for this glitch. For the ninth glitch unpublished timing data start 7 minutes after the glitch (Flanagan 1991).

The evidence is now quite strong that pulsar glitches and the subsequent changes in pulsar period (postglitch relaxation) reflect changes in the angular momentum distribution inside the neutron star. No systematic changes in the electromagnetic signature of a pulsar were observed to correlate with glitches up to the eighth glitch of the Vela pulsar. This is the only glitch for which there may be evidence for a change in the dispersion measure in one set of observations (Hamilton et al. 1989; McCulloch et al. 1990), which might imply a glitch-induced change in the structure of the magnetosphere and perhaps in the electromagnetic torque. For microglitches, those glitch-induced changes may result in pulsar timing noise (Cheng 1987a, b). The glitches and their subsequent relaxation therefore provide a valuable tool for probing the neutron star inte-

[1] Present address: Department of Physics, University of Illinois at Urbana-Champaign, Urbana, IL 61801

rior. We shall pursue the viewpoint that the glitches, at least those of the large size ($\Delta\Omega/\Omega \sim 10^{-6}$) and frequency (roughly every 2–3 yr) observed in the Vela pulsar, are due to the sudden unpinning and outward motion of large numbers ($\sim 10^{11}$) of vortex lines in the crustal neutron superfluid which are pinned there to the lattice of neutron-rich nuclei (Pines 1971; Anderson & Itoh 1975). The conservation of angular momentum in the crustal neutron superfluid relates the observed increase $\Delta\Omega_c$ in the rotation rate of the crust (of effective moment of inertia I_c) to the decreases $\delta\Omega_i$ in the superfluid rotation rate in the various regions of superfluid, with moments of inertia I_i, through which unpinned vortices move at a glitch:

$$I_c \Delta\Omega_c = \sum_i I_i \delta\Omega_i \,. \tag{1}$$

The effective crust moment of inertia I_c denotes all parts of the star that couple to the outer crust on time scales short compared to the observational resolution of a glitch ($\lesssim 2$ minutes for the eighth glitch). I_c includes the superfluid in the core of the star (Alpar, Langer, & Sauls 1984c; Alpar & Sauls 1988) and thus the bulk of the total moment of inertia, while $\sum_i I_i$ was found to be 10^{-2} to 10^{-3} of the star's total moment of inertia in previous work (Alpar et al. 1984b) as well as the fits presented here.

Over the years, vortex creep theory, a model of the postglitch relaxation in terms of the rotational dynamics of a superfluid with vortex pinning inside the neutron star crust, has been developed and applied to data from several pulsars (Alpar et al. 1984a, b; Alpar, Nandkumar, & Pines 1985; Alpar et al., 1988; Cheng et al. 1988). In this theory the vortex-lattice interaction is modeled in terms of thermally activated vortex motion over discrete pinning configurations. The theory provides a means of extracting information on the structure and temperatures of neutron stars as well as detailed information on the physical characteristics of the pinned crustal neutron superfluid (Pines & Alpar 1985). In vortex creep theory, the response of a given region of the star can be either linear or nonlinear, depending on how close the lag, ω, in the angular velocity of the pinned crustal superfluid is to the critical lag, ω_{cr}, at which unpinning will take place in that region; the theory also predicts an evolution in the nature of a pulsar's dynamical relaxation in conjunction with its thermal evolution (Alpar, Cheng, & Pines 1989). The linear response produces the various components of exponential relaxation observed in the postglitch timing data, while the nonlinear response is essential for explaining the long time scale behavior and the angular momentum exchange including the glitches. It is an attractive feature of the vortex creep model that both types of observed postglitch behavior are obtained as two regimes of the same physical model.

A different aspect of the interaction of vortex lines with the lattice is the coupling of vortex motion and excitations with phonons of the lattice (Jones 1990a, b, c, 1991; Bildsten & Epstein 1989). This approach describes vortex motion with respect to the lattice at temperatures that are too low for thermal activation, and also the rapid scattering of unpinned vortices during glitches (Epstein & Baym 1992; Jones 1992; Henis & Shaham 1981), aspects of vortex motion that are not treated by the vortex creep model. The exponential relaxation part of the postglitch response (which we interpret as the linear response in the vortex creep model) has also been explained in terms of vortex-phonon scattering (Jones 1990a, b, c, 1991, 1992), with vortices almost moving with the superfluid, at a small velocity with respect to the lattice.

The microscopic physics of vortex pinning is a difficult problem with many uncertainties. We use estimates of the pinning energy based on a comparison of superfluid condensation energies inside and outside the nuclei (Alpar 1977; Anderson et al. 1982; Alpar et al. 1984a). A Ginzburg-Landau treatment (Epstein & Baym 1988) gave large pinning energies implying energy dissipation rates in excess of observational upper limits (Alpar et al. 1987). We believe this was an overestimation resulting from a problematic application of the boundary conditions. On a different extension of the pinning model, the effects of tension in vortex lines were taken into account by Chau & Cheng (1991) and by Baym, Link, & Epstein (1992), yielding effective pinning energies within the same range as the initial estimates. The pinning energy enters as a parameter in the dynamical model of vortex creep applied in this paper. We model the pinning energy in terms of a lowest order estimate with a scale factor to represent uncertainties in the actual pinning strength.

The initial attempt to use vortex creep theory to analyze the postglitch behaviour of the Vela pulsar (Alpar et al. 1984b) was confined to data from its first four glitches; since there was considerable uncertainty in the actual dates of these glitches, the conclusions reached there (on the basis of calculations which took only nonlinear response into account) were of necessity more qualitative than quantitative. The fact that two glitches have now been observed within minutes of the time of occurrence (including glitch nine for which data have not been published yet), while two others have been caught within less than a day, brings sharply into focus the short-term response of the pinned crustal superfluid to a glitch, and the observational data on the four post-1984 glitches provide a much-needed complement to that obtained for the first four glitches. The aim of the present paper is to evaluate the postglitch relaxation data following the first eight glitches of the Vela pulsar in a consistent framework and to explore the long-term angular momentum balance.

Our basic approach is the following:

1. We first examine the extent to which vortex creep theory provides a consistent phenomenological description of the observations following all eight glitches, using a "minimalist" phenomenological model which is subject to the constraint that the nature of the physical response of a given pinning region should be the same after each glitch.

2. We next consider the physical location of the distinct pinning regions identified in the postglitch data (i.e., did vortices pass through in a glitch, or not?), the character of the dynamical response (linear or nonlinear?) to the glitch, and the implications of these conclusions for the pinning characteristics (strong, weak, or superweak?) of the region in question. We demonstrate that vortex creep theory provides an answer to many of these questions and so makes possible a consistent physical picture of both where glitches occur, and of postglitch behavior.

3. We then examine the extent to which glitches permit pulsars to be used as cosmic hadron physics laboratories (Pines 1991), that is, the extent to which the information on postglitch behavior derived from observation can be used to constrain microscopic calculations of the crustal neutron superfluid energy gap, pinning energies, and the neutron star equation of state.

We find that all eight postglitch data sets can be described in terms of three distinct components of short and intermediate

time scale exponential relaxation, characterized by relaxation times of 10 hr, $3^d.2$, and 32^d, followed by a long-term recovery of the glitch-induced change in the spin-down rate that is linear in time. We show that the short-to-intermediate time scale exponential relaxation reflects the linear response of vortex creep in regions of the stellar crust through which no sudden vortex motion occurred at the time of the glitch, while the long-term response linear in time represents the nonlinear response of regions through which there is a sudden motion of vortices at the time of a glitch. We demonstrate that there must exist as well regimes of the pinned crustal superfluid which play a significant role in determining the angular momentum balance, despite the fact that the regions in question cannot sustain a vortex creep current. We explain the tendency of glitches to leave permanent spin-up remnants and find that, on average, the theoretically expected interglitch intervals agree well with those observed.

Our conclusion that the most likely physical origin of the 32^d response is a region of superweak pinning in the vicinity of the transition to a regime of linear creep enables us to constrain the magnitude and density dependence of the neutron superfluid energy gap for the density region, 7×10^{13} g cm$^{-3} \lesssim \rho \lesssim 1.2 \times 10^{14}$ g cm^{-3}, taking into account present uncertainties in the estimates of pinning energies and the criterion for the transition from weak to superweak pinning. We find that for physically reasonable choices of pinning energies and the transition criterion, a portion of the family of possible gap functions obtained in the recent microscopic calculations of Ainsworth, Pines, & Wambach (1989) is consistent with these constraints. We are also able to obtain a firm lower bound on the moment of inertia of the crust of the neutron star; our fit to the largest glitch observed to data, that of 1978 July 3, requires that the inertial moment of the observed pinned crustal neutron superfluid be at least 2.4% of the stellar inertial moment. Since the total crustal moment of inertia must be larger than this, our limit already serves to rule out neutron star models built upon a soft equation of state for neutron matter at densities comparable to or greater than that of nuclear matter (Pandharipande, Pines, & Smith, 1976).

In § 2 we give a brief summary of vortex creep theory and introduce the "minimalist" phenomenological model which we show in § 3 is capable of providing a consistent fit to all eight sets of postglitch observational data. Section 4 contains a discussion of the physical basis for the linear response to the glitch in the form of fast and intermediate time exponential decays of part of the glitch, and the constraints this response places on the description of the pinned crustal neutron superfluid. We consider the long-term behavior of the pinned crustal superfluid in § 5, and discuss our conclusions in § 6.

2. SUMMARY OF VORTEX PINNING AND CREEP

In vortex creep theory it is assumed that there exist several physically distinct regions of different pinning strengths (Anderson et al. 1982; Alpar et al. 1984b.) Moreover, for a particular region it is shown that depending on the temperature, the thermal creep of vortices can be in either a linear or a nonlinear dynamical regime (Alpar et al. 1989). The pinning energy E_p is the gain in energy when a nucleus is inside the normal matter core of a vortex line. It is estimated as

$$E_p = \frac{3}{8\pi}\left[\left(\frac{\Delta^2 n}{E_F}\right)_{\rm out} - \left(\frac{\Delta^2 n}{E_F}\right)_{\rm in}\right] V , \qquad (2)$$

where Δ, E_F, and n are the gap, the Fermi energy, and the number density of superfluid neutrons inside and outside a nucleus, and V is the nuclear volume. When a vortex line is pinned and moving with the lattice, pinning forces sustain the velocity difference between the vortex line and the lattice. The maximum (critical) lag, $\omega_{\rm cr}$, between the rotation rates of the superfluid and of the crust lattice that can be sustained by the pinning energy E_p is

$$\omega_{\rm cr} = \frac{E_p}{\rho \kappa r b \xi} , \qquad (3)$$

where ρ is the superfluid density, κ is the vorticity quantum, and r is the distance from the rotation axis of the star. The distance between successive pinning sites along a vortex line, which we denote by b, is an important parameter; it is of the order of b_z, the lattice spacing, in the "strong" pinning regions, but longer in the "weak" and "superweak" pinning regions.

If E_p exceeds the binding energy of a nucleus to its equilibrium site in the lattice, we call this "strong pinning." A vortex line will then be able to dislodge nuclei and pin to a nucleus in every unit cell of the lattice, so that the distance between successive pinning sites along the vortex line is simply the lattice spacing. Observational upper limits (Alpar et al. 1987) indicate that such strong pinning is not present in any substantial parts of the crust superfluid. We shall therefore not pursue the alternative of strong pinning.

When pinning forces are not strong enough for a vortex line to dislodge nuclei, it is expected to pin only to those nuclei that it encounters geometrically along its orientation in the lattice. With the superfluid coherence length $\xi = (2/\pi)(E_F/k_F\Delta)$ defining the radius of the vortex line core, the distance b between successive pinning sites along a vortex line is

$$b = b_z^3/\pi\xi^2 , \qquad (4)$$

where b_z^3 is the lattice volume per nucleus.

At higher densities in the inner crust, where the superfluid gap decreases and the radius of vortex cores (the coherence length ξ) increases, vortex cores become large enough to include several lattice sites simultaneously. Hence at $\xi \gtrsim b_z/2$, the nature of pinning must change, because the pinning configuration will now change only slightly if a vortex line is displaced in the lattice; the effective strength of pinning may be expected to diminish, probably by some large factor. We do not at present have any way of estimating pinning parameters in this "superweak" pinning regime. In particular it is not known whether the transition involves only an increase in the distance b between pinnings along the vortex line, with each effective pinning site providing the energy gain E_p of one nucleus, or whether there is also a reduction to an effective pinning energy, $E_p' < E_p$. In § 4 we present a possible consistent interpretation of the postglitch data with the response of several superweak pinning regions. The observed relaxation time scales we associate with superweak pinning are then used to infer superweak pinning parameters.

Vortex creep theory models the dynamical coupling between the crust and the pinned superfluid in terms of the thermal flow (creep) of vortices. The observed spindown $\dot{\Omega}_c$ of the neutron star crust obeys the equation

$$I_c \dot{\Omega}_c = N_{\rm ext} + N_{\rm int} = N_{\rm ext} - \sum_i I_i \dot{\Omega}_i , \qquad (5)$$

where I_c is the effective moment of inertia of the crust including all parts of the star that couple to the crust on shorter than observable time scales, N_{ext} is the external pulsar torque, and N_{int} is the total internal torque coupling various parts of the crustal superfluid, with moments of inertia I_i and spindown rates $\dot{\Omega}_i$, to the crust. The internal torques depend on the characteristic pinning energy scale E_p, the temperature T of the neutron star interior, and on the lag $\omega \equiv \Omega_s - \Omega_c$ between the rotation rate of the superfluid, Ω_s, and that of the crust, Ω_c (Alpar et al. 1984a). This theory has a steady state solution with $\dot{\Omega}_s = \dot{\Omega}_c$, achieved at some value ω_∞ of the lag.

There are two different regimes of dynamical response. A linear regime occurs when the temperature is sufficiently large compared to the pinning energy that the steady state corresponding to the external torque can be achieved with a small lag. Each part of the superfluid that responds in the linear creep regime will have a simple exponential relaxation as a function of time, with an amplitude that is linear in the perturbation of ω affected by the glitch in that particular region. The linear response from some region i of the superfluid will show up in the postglitch perturbation $\Delta\dot{\Omega}_{c,i}(t)$ of the spin-down rate as a term with an exponential decay time $\tau_{l,i}$ characteristic of that region (Alpar et al. 1989):

$$\Delta\dot{\Omega}_{c,i}(t) = -\frac{I_i}{I}\frac{\delta\omega_i(0)e^{-t/\tau_{l,i}}}{\tau_{l,i}} . \quad (6)$$

Here I_i is the moment of inertia of the region i, I is the total moment of inertia of the star, and $\delta\omega(0)$ is the perturbation, caused by the glitch, to the lag $\omega = \Omega_s - \Omega_c$ in that region. In a glitch, $\Omega_c \to \Omega_c + \Delta\Omega_c$ and, in those regions i where vortex motion associated with the glitch reduces the local superfluid rotation rate, $\Omega_s(r) \equiv \Omega_i \to \Omega_i - \delta\Omega_i(0)$. The reduction in the lag ω_i is then $\delta\omega_i(0) = \delta\Omega_i(0) + \Delta\Omega_c$. The characteristic decay time τ_l in the linear regime is related to pinning parameters and temperature through

$$\tau_l = \frac{kT}{E_p}\frac{\omega_{cr} r}{4\Omega v_0}\exp\frac{E_p}{kT} , \quad (7)$$

where Ω is the star's rotation rate, and $v_0 \sim 10^7$ cm s^{-1} is a typical velocity of microscopic vortex motion.

When the temperature is sufficiently low compared to the pinning energy E_p a large steady state lag $\omega_\infty \lesssim \omega_{cr}$ is needed for the superfluid to spin down at the steady rate appropriate to the external torque. In this regime the response of the spin-down rate $\Delta\dot{\Omega}_{c,k}(t)$ has a Fermi-function dependence on time (Alpar et al. 1984a, b) and a nonlinear dependence on the glitch-induced initial offset $\delta\omega(0)$ from steady state. The typical contribution of a nonlinear creep region k to the relaxation of the observed perturbation in $\dot{\Omega}_c$ is

$$\frac{\Delta\dot{\Omega}_{c,k}(t)}{\dot{\Omega}_c}(t)\ \text{(nonlinear)} = \frac{I_k}{I}\left\{1 - \frac{1}{1 + [\exp(t_{0,k}/\tau_{n,k}) - 1]\exp(-t/\tau_{n,k})}\right\} , \quad (8)$$

where I_k is the moment of inertia in that region of superfluid, $t_{0,k} \equiv \delta\omega_k(t = 0)/|\dot{\Omega}|$ describes the initial postglitch offset in ω, and the relaxation time τ_n is

$$\tau_n = \frac{kT}{E_p}\frac{\omega_{cr}}{|\dot{\Omega}|} . \quad (9)$$

Creep will be linear if $\tau_l < \tau_n$, and nonlinear if $\tau_n < \tau_l$. The transition from linear to nonlinear response takes place at $\tau_n = \tau_l$, which occurs at a value of the pinning energy (Alpar et al. 1989)

$$(E_p/kT)_{tr} = 35.5 + \ln(t_{s,6}) + \ln(v_{0,7}/r_6) = 31 , \quad (10)$$

where $t_{s,6} = \Omega/2|\dot{\Omega}|$ denotes the spindown age of the pulsar in units of 10^6 years and the last equality gives a numerical value for the Vela pulsar obtained by setting $v_{0,7}/r_6$ to 1. This transition corresponds to $\tau_n = \tau_l \approx 1000$ days in the Vela pulsar. Regions with weaker E_p will respond linearly and those with stronger E_p will respond nonlinearly.

We emphasize that the classification of a particular part of the pinned superfluid as having "weak" or "superweak" pinning depends on the distribution of the pinning parameters E_p and b there and is independent of the classification of dynamical response as linear or nonlinear creep; the latter depends on a comparison of temperature, external torques, and pinning parameters. A weak or superweak pinning region can be in either of the linear or nonlinear creep regimes. As a framework for discussing the different combinations of response that give good fits to the data, we show in Figure 1 linear and nonlinear regime relaxation times for the Vela pulsar based on weak pinning parameters (Alpar et al. 1989), adopting for definiteness a temperature of 11 keV for the neutron star interior. This temperature estimate is obtained

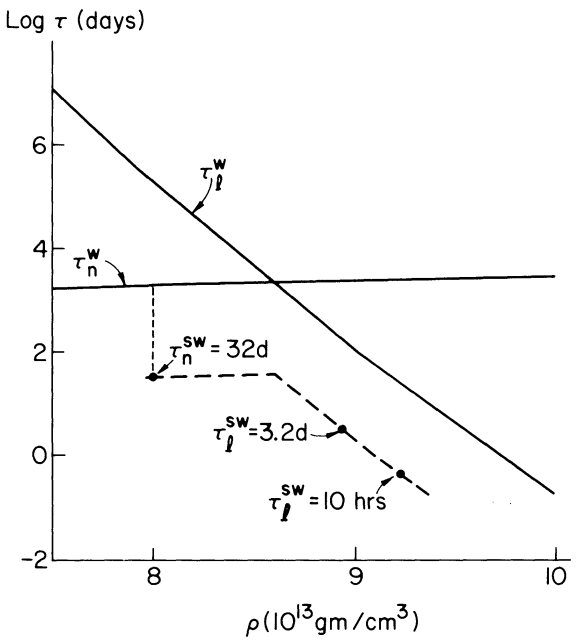

FIG. 1.—The relaxation times for linear and nonlinear regimes of vortex creep, calculated for a temperature $kT = 11$ keV for the interior of the Vela pulsar, using weak pinning parameters with $\gamma = 0.5$. Log [τ (days)] is plotted against the density ρ in units of 10^{13} g cm^{-3}. The regime with the shorter relaxation time prevails. For $\rho < \rho^{sw}$, the shortest relaxation time, $\sim 1000^d$, is associated with the nonlinear response of a weakly pinned region. At $\rho^{sw} = 8 \times 10^{13}$ g cm^{-3}, within the nonlinear creep region, a transition to superweak pinning takes place; for $\rho \geq \rho^{sw}$, $\tau_n \cong 32^d$. For $\rho > \rho^{tr} = 8.6 \times 10^{13}$ g cm^{-3}, the creep becomes linear. The dashed lines give τ_n and τ_l for superweak pinning schematically. These are obtained by choosing the effective pinning distance b to give $\tau_n = 32$ days at ρ^{sw}. The 10 hr, 3^d2, and 32^d relaxation times are to be associated with regions labeled with these relaxation times. The gap function, $\Delta(\rho)$, used in these calculations is shown in Fig. 4*a*. ρ^{sw} is calculated using $\gamma' = 1$.

from observational limits on the surface temperature (Ögelman & Zimmermann 1989) assuming the surface-interior temperature relation of Gudmundson, Pethick, & Epstein (1982). Superweak pinning is treated only qualitatively in this framework, and its parameters are chosen to give a 32^d relaxation time.

The combined nonlinear response from regions k, each of which contributes a response determined by its particular offset time $t_{0,k}$, as in equation (8), depends on the distribution of postglitch initial conditions $t_{0,k}$ throughout the nonlinear response regions of the superfluid. If $t_{0,k} = \delta\omega_k(0, r)/|\dot{\Omega}|$ is uniform over a region with a total moment of inertia I_B, which supported steady state vortex creep prior to the glitch, then for times t after the glitch less than $t_{0,k}$, the nonlinear response would be a constant shift in $\dot{\Omega}_c$, $\Delta\dot{\Omega}_c/\dot{\Omega} = I_B/I$, and this shift in $\dot{\Omega}_c$ would be recovered in a time interval of the order of τ_n around $t_{0,k}$, where τ_n is the nonlinear relaxation time in region B. If $\delta\omega_k(0, r)$ varies linearly with position r in some parts of the nonlinear response region with total moment of inertia I_A so that $0 < t_{0,k} < t_0$, where t_0 is the maximum offset time corresponding to the maximum of $\delta\omega_k(0, r)$, then an initial shift $\Delta\dot{\Omega}_c/\dot{\Omega} = I_A/I$ is recovered linearly in time starting at $t = 0$ right after the glitch. This is because the moment of inertia that has recoupled by time t, i.e., the moment of inertia of those regions k with $t_{0,k} < t$, is increasing linearly with time t. Such linear dependence of $\delta\omega_k(0, r)$ on r corresponds to a uniform density of vortices unpinned and repinned at the time of the glitch; it is a lowest order model for $\delta\omega(0, r)$ that is motivated by the long-term recovery of the Vela pulsar, in which $\Delta\dot{\Omega}_c$ has a linear dependence on time. Note that many separate such regions would collectively give a response also linear in time. For this model of nonlinear response to give a simple $\Delta\dot{\Omega}_c(t) \propto t$ term, it is sufficient to have $\tau_n \ll t_0$.

In the course of our 1984 analysis of the first four glitches of the Vela pulsar, we proposed a "minimalist" model for a glitch in which catastrophic vortex unpinning occurs in the vicinity of a boundary between two distinct pinning regions, with vortices moving outward after the glitch and repinning elsewhere in the star. We shall see that this model, suitably interpreted, contains all the elements required to explain the postglitch behavior for all eight glitches. The proposed form of $\delta\omega(0, r)$ after the glitch is given in Figure 2. This corresponds to a uniform vortex density which unpins from a region A1 and repins in a region A2. In between, there is (possibly) a region B through which vortices move at the glitch, but no vortices unpin or repin; then $\delta\omega(0, r)$ is uniform through region B. Figures 3*a* and 3*b* show the response in $\Delta\dot{\Omega}_c$ to such a perturbation, if vortex creep operating in these regions prior to the glitch was stopped as a result of the perturbation.

Integrating contributions from linear and nonlinear creep regimes, we find that the general form of postglitch response is

$$\frac{\Delta\dot{\Omega}_c(t)}{\dot{\Omega}} = \int \frac{dI_l(r)}{I} \frac{\delta\omega_l(0)e^{-t/\tau l}}{|\dot{\Omega}|\tau_l} + \int \frac{dI_{nl}(r)}{I} \times \left\{1 - \frac{1}{1 + [\exp(t_0(r)/\tau_n) - 1]\exp(-t/\tau_n)}\right\} + \left(\frac{I_A}{I} + \frac{I_B}{I}\right) \times \theta(t) - \frac{I_A}{I}\frac{t}{t_g}\theta(t)\theta(t_g - t) - \left(\frac{I_A}{I} + \frac{I_B}{I}\right)\theta(t - t_g) . \quad (11)$$

This equation gives the form of the model fits we have applied to postglitch timing behavior after the eight Vela pulsar glitches to date. For reasons to become clear in the discussion section, we have labeled the offset time t_0 associated with regions A and B as t_g. The response given in equation (11) is a general form which allows for combinations of the different

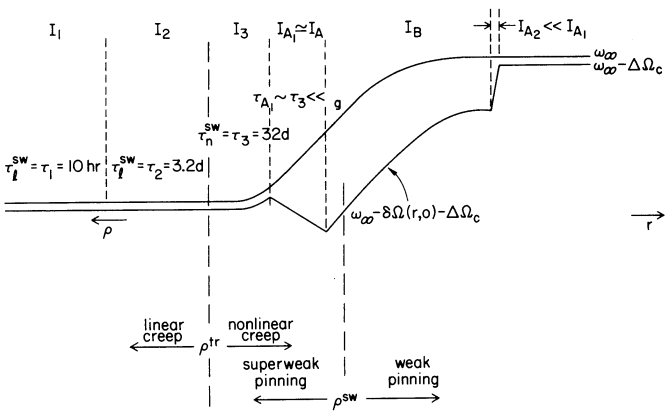

FIG. 2.—A "minimalist" toy model of a glitch which indicates the relative positions of the vortex unpinning regions A_1 and repinning regions A_2 labeled jointly as regions A, and the vortex scattering (vortex depletion) regions B in the crustal superfluid, together with the perturbation $\delta\Omega(0, r)$ to the superfluid rotation rate produced by vortex motion at the time of a glitch. The distance from the rotation axis increases to the right and the density to the left. The positions of the various components of postglitch response, 1, 2, 3, A, and of the transitions between superweak and weak pinning (at ρ^{sw}), and between linear and nonlinear creep (at ρ^{tr}) are indicated. In "passive" regions, through which vortices do not move, the response of the superfluid to a glitch is set by $\delta\omega = \Delta\Omega_c$. In the active region, vortex motion transfers angular momentum at glitches, so that immediately after a glitch $\delta\omega = \delta\Omega(r, 0) + \Delta\Omega_c$.

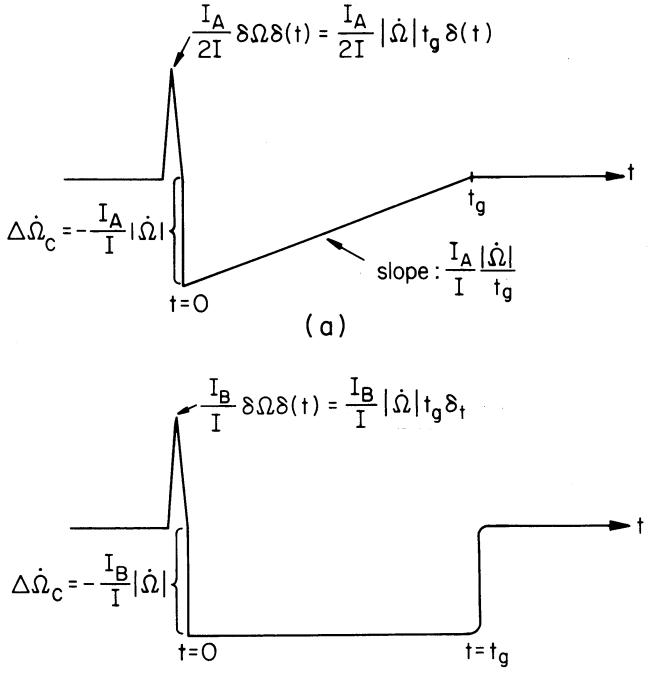

FIG. 3.—(*a*) The form of the $\Delta\dot{\Omega}_c(t)$ expected from the uncoupling and recoupling of vortex creep in regions A but not in regions B. Such behavior is observed after each glitch. (*b*) The expected form of $\Delta\dot{\Omega}_c(t)$ if vortex creep were sustained also in regions B, uncoupling at a glitch and recoupling subsequently. Such behavior, characterized by the recoupling signature at $t \sim t_g$, is not observed.

types of linear and nonlinear response of vortex creep that we have developed and applied to the Vela pulsar and other glitching pulsars. We do not expect all terms in this general model to be present in a comprehensive fit to the eight Vela pulsar glitches. It is our aim here to eliminate some of the terms and so to reduce the response function to the simplest combination that can be applied to all eight glitches using the same or similar parameter values and at the same time allowing a consistent physical interpretation.

We shall see that the simplest good fits with consistent parameters for eight glitches have the following features:

1. The integrated linear response in the first term of equation (11) is replaced by a sum of three simple linear response terms involving regions through which no vortex motion occurs. Two of these, the 10 hr and the 3^d2 response, correspond to regions of superweak pinning through which no vortices move; we assume that all eight glitches originate in regions of similar density, and ask whether *these two regions respond in the same way*, i.e., with the same inertial moment and the same relaxation time, *after each glitch.* Comparing the results of independent fits to the separate postglitch data set with fits requiring the same response after each glitch we find that the goodness of fits of the latter type ("consistent" fits) is comparable to the best fits with different relaxation parameters after each glitch, and thus conclude that it is indeed tenable to assume that there are two regions of the star that respond the same way after every glitch (to correspond to regions of superweak pinning through which no vortices move). The third linear response term can likewise be fitted with the same relaxation time $\tau_3 = 32^d$ after each glitch, while it is not possible to find a good fit with the same inertial moment in this component after each glitch. We associate this response with a region which lies close to the boundary separating the superweak and weak pinning regimes. Because the exact location of the catastrophic vortex unpinning varies from one glitch to the next, the magnitude of the inertial moment which characterizes this 32^d response changes from one glitch to the next.

2. Nonlinear response exhibiting the full Fermi function behavior is not present, so the second term in equation (11) depicting a combination of such Fermi function responses is not warranted (other than giving rise to a term proportional to t, which, as we discuss below, is interpreted as a particular combination of nonlinear Fermi function responses).

3. The remaining terms depicting the long time scale nonlinear response in the form of an offset in $\dot{\Omega}_c$ and a gradual recoupling linearly in t are present, but they have a particularly simple form in terms of the moments of inertia I_A and I_B. Figures 3*a* and 3*b* depict possible forms of the long-term response. We find that a simple and consistent interpretation of all Vela glitches is obtained if the regions B contribute only to sudden vortex motion and angular momentum transfer at the time of a glitch, but not to any offset in $\dot{\Omega}_c$ (see Fig. 3*a*), a situation which occurs when the regions B do not participate in vortex creep either before or after glitches. In such regions B, vortex motion can occur only as a consequence of sudden unpinnings at glitches. Since these never contribute to $\dot{\Omega}_c$ through a continuous internal torque, they will not appear in equation (11), though they will contribute to the angular momentum balance and to the observed glitch magnitude $\Delta\Omega_c$. Thus the long time scale nonlinear response is represented only by regions A in which vortex creep uncouples at the time of a glitch, producing a sudden decrease in $\dot{\Omega}_c(t)$ which then recovers as a linear function of time.

With this model, the angular momentum balance, equation (1), reads

$$I_c\,\Delta\Omega_c = (\tfrac{1}{2}I_A + I_B)\delta\Omega\ ; \tag{12}$$

the factor $\frac{1}{2}$ appears with I_A because for the regions A, $\delta\Omega$ increases linearly, $0 < \delta\Omega(r) < \delta\Omega$, so that it is represented on the mean by $\frac{1}{2}\delta\Omega$. Recall that I_c is almost the total moment of inertia of the star.

3. METHOD OF DATA FITTING

In the last section we discussed various possible modes of response within the framework of the vortex creep model. In the absence of a firm understanding of the physics of pinning, we look to the data for hints about the nature of pinning. Our method of model fitting involves minimizing the sum of the squares of the residuals (the χ^2) between the model curve and the data points, defined as

$$\chi^2 = \sum_i \left[\frac{\Delta\dot{\Omega}_c(t = t_i, \alpha_1, \alpha_2, \ldots, \alpha_N) - \Delta\dot{\Omega}_{c,i}}{\sigma_i}\right]^2, \tag{13}$$

where $\Delta\dot{\Omega}_c(t_i, \alpha_1, \ldots, \alpha_N)$ is the theoretical value of the change of the rotation rate at t_i, α_j ($j = 1, 2, \ldots, N$) are the model parameters which can be determined via the minimization process, $\Delta\dot{\Omega}_{c,i}$ is the observed change of rotation rate at t_i, and σ_i is the error bar of the observed $\Delta\dot{\Omega}_c(t_i)$. Where measurement errors are dominated by timing noise, as in the timing fits of Cordes et al. (1988), we adopt the amplitude of the timing residuals as representative of the overall error bars. A program for nonlinear least-squares fitting was written in C Language of IBM PC. (The C program and user guide are available from H. F. C. on request.) In the program, three algorithms are provided: the Gauss method; the Levernberg-Marquardt method; and the method of steepest descent. (For the theory of fitting, see Press et al. 1987.) Fits were performed for postglitch data sets of individual glitches, as well as for the entire data sets. The comparison of the different fits and the model parameters are discussed below.

The procedure of finding the best parameters goes through several steps:

1. Make an initial guess of the parameters.
2. Use the Gauss method and the Levernberg-Marquardt method to find the best values of the parameters.
3. Improve the parameters by using the method of steepest descent.

Making the initial guess can be done by trial and error. A set of good initial parameters not only makes the program converge to the best fit faster, but also helps it avoid getting trapped in some local minimum of the complicated N-dimensional parametric manifold. The rough values of some parameters can be obtained by doing "prefits" for subsets of the data. For example, at late times, we know that the long time scale component dominates in the fitting function. Thus we simply fit this term to the latest data points at late times after the glitch to obtain a reasonable guess for some parameters of the entire fitting function (i.e., I_A/It_g). In many cases, inspecting the data by eye, one can tell that there is a fast relaxation component. It is easy to obtain this short characteristic time by fitting a simple exponential function. We can also guess at likely values of the parameters from theory. For example, the moment of inertia of the pinning regions must be around 10^{42}–10^{43} g cm^2 with all reasonable equations of state.

In § 2, we have discussed possible modes of postglitch relax-

ation within the framework of the vortex creep model. On the shortest time scales, a simple exponential relaxation with $\tau_1 \sim$ 10 hr is required by the data following glitch 8, when analyzed in short spans (Flanagan 1990a, b). For glitch 8, information on the earliest relaxation following the glitch is available, as this glitch occurred during an observing session. The shortest time scale relaxation for all glitches is assumed to be represented by that observed after glitch 8. The 10 hr time scale from Flanagan's data fits was adopted as the shortest time scale response. Although the fifth and sixth glitches were also caught within 1 day (McCulloch et al. 1981, 1983; Hamilton et al. 1982) the postglitch data fits do not have the resolution to fit for time scales of order 10 hr.

At the longest time scales in all postglitch data sets, the relaxation has the form $\Delta\dot{\Omega}_c(t) \sim t$. In addition, two intermediate time scales of relaxation are present in the data. Attempts to fit all postglitch data sets with the same model indicate that combinations of simple exponentials yield equally good fits when compared with integrals like the first term in equation (11), which describes a composite response in the linear regime, or with nonlinear response terms like equation (8) to account for the intermediate time scales $\approx 30^d$. For simplicity we looked for the best fit with the minimum number of exponential relaxation terms, plus the long-term response $\Delta\dot{\Omega}_c(t) \sim t$. Independent fits to the individual postglitch data sets yielded two components of intermediate time scale exponential relaxation, with relaxation times τ_2 ranging between 3^d and $3\overset{d}{.}5$, and τ_3 ranging between 29^d and 39^d. Requiring the same values of τ_2 and τ_3 in all postglitch data sets gave best-fitting values of $\tau_2 = 3\overset{d}{.}2$ and $\tau_3 = 32\overset{d}{.}7$. The best fit with a common set of parameters for all postglitch data was found by trial and error in the parameter space common to the range of best fits to individual postglitch data sets.

In the fits to $\Delta\dot{\Omega}_c(t)$ the coefficients of the exponential relaxation terms $a_i \exp - t/\tau_i$ have the form $a_i = I_i/I[\Delta\Omega_c(0)/\tau_i \exp - \Delta/\tau_i]$ describing the response of a region with moment of inertia I_i and relaxation time τ_i through which no vortex motion occurred at the glitch, so that the response is to the crust's observed spin-up $\Delta\Omega_c(0)$ at the glitch. The parameter Δ (days) is the time of the first postglitch observation from the unknown occurrence time of the glitch. For the later glitches the maximum uncertainty Δ_{max} in the glitch occurrence time is small, with $\Delta = \Delta_{max} = 0$ for glitch 8, while for the earlier glitches there is considerable uncertainty, $\Delta \leq \Delta_{max}$ (see Table 2). The exponential relaxation with $\tau_1 = 10$ hr is observed only in glitch 8 and we assume I_1/I has the same value for all glitches. The amplitude a_2 of the relaxation with $\tau_2 = 3\overset{d}{.}2$ gives I_2/I for the eighth glitch since $\Delta = 0$ for that glitch. It turns out that fitted values of a_2 for the other glitches allow the same value of I_2/I for all glitches with corresponding choices of $\Delta < \Delta_{max}$ for the individual glitches. This does not prove possible for the I_3/I once the Δ values are chosen to have a single I_2/I value for all postglitch data. Thus the hypothesis that the same moments of inertia I_1/I and I_2/I are involved, representing the same responding regions after each glitch is tenable but may be an artifact of the uncertainty in glitch date in the earlier glitches. The variability of I_3/I is interpreted as showing that this is the region where vortex motion starts, and its location changes from glitch to glitch. Thus in our fits it is τ_2 and τ_3 that can be fitted directly with the same values for all postglitch data sets (τ_1 being chosen from the fit to glitch 8 alone). In Table 1 we compare the fits produced by the best-fitting all-glitch choice of the τ's with the individual best fits to the separate postglitch data sets. χ^2 values for the best fit and the consistent fit are given for the individual postglitch data sets, together with the number of degrees of freedom for each data set. We note that the consistent fit compares well with the best fit in each data set. Now adding the important point that the consistent fit parameters $\tau_2 = 3\overset{d}{.}2$ and $\tau_3 = 32\overset{d}{.}7$ actually compare well in independent fits to all postglitch data sets, we see that our hypothesis that the same relaxation times $\tau_2 = 3\overset{d}{.}2$ and $\tau_3 = 32\overset{d}{.}7$ are present after all glitches is consistent with the observational data. Confirmation of the same statement for τ_1 and for the moments of inertia requires analysis of data from glitch 9 and future glitches that are caught at the time of occurrence ($\Delta = 0$). Table 1 also shows, for both the best individual fits and the consistent fit, the amplitudes $a_i = I_i/I$ $\Delta\Omega_c(0)/\tau_i \exp -\Delta/\tau_i$ for the exponential relaxation as well as the slope $\Delta\dot{\Omega}/|\dot{\Omega}|$ and intercept $\Delta\dot{\Omega}$ (0) (long term)/$|\dot{\Omega}|$ of the long-term response $\Delta\dot{\Omega}_c \propto t$. Table 2 gives the parameters of the consistent fit, and Figures 4*a*–4*h* show this consistent fit on the individual postglitch data sets.

4. DISCUSSION

4.1. *The Fast and Intermediate Time Scale Response*

In the Vela pulsar, as in other relatively young pulsars, the faster components of postglitch relaxation can reflect combinations of linear and nonlinear creep response (Alpar et al. 1989). As noted above, a combination of three linear regime terms (simple exponentials) is adopted as it is the simplest among comparably good models (in conjunction with long time scale behavior to be discussed below) that give good fits with the same model parameters to all eight postglitch data sets.

The $3\overset{d}{.}2$ relaxation common to all glitches and the 10 hr relaxation time resolved after glitch 8 establish unambiguously the presence of two time scales associated with the linear regime. Were the response with $\tau = 10$ hr or $\tau = 3\overset{d}{.}2$ in the nonlinear regime, even the minimum offset time $t_0 = \Delta\Omega_c/|\dot{\Omega}| \sim 10^d$ would give a typical Fermi function behavior with no recoupling until t is within τ of t_0; such behavior is not observed. The regions responsible for this short time scale response can also be identified; the response reflects the relaxation of vortex creep in those superfluid regions through which no vortex motion occurred at the time of the glitch. To see this, we note that the amplitudes of the exponential relaxation terms in $\Delta\dot{\Omega}_c(t)$ have the general form $(I_i/I)\ \delta\omega_i(0)/\tau_i$. For regions where no vortex motion occurred, $\delta\omega_i(0) = \Delta\Omega_c$, and the amplitude is $(I_i/I)\ \Delta\Omega_c/\tau_i$. On the other hand, if vortex motion did occur, $(I_i/I)\ \delta\omega_i(0) \sim (I_i/I)\ \delta\Omega_i(0) \sim \Delta\Omega_c$, on making use of the angular momentum balance conditions, equation (12). Since the former case, with the much smaller amplitude $(I_i/I)\ (\Delta\Omega_c)/\tau_i$ is observed for both the short time scales, we are able to conclude that these must be associated with regions through which no vortex motion occurred.

We next consider whether the intermediate 32^d time scale reflects a linear or a nonlinear region of vortex creep. Suppose it represents a region i in which the creep is nonlinear. If so, the region must be one where no vortex motion occurred at the glitch, for which $t_0 = \Delta\Omega_c/|\dot{\Omega}|$. [Had vortex motion occurred, t_0 would be equal to $\delta\Omega_i(0)/|\dot{\Omega}|$, which would imply a wait of several years before any recoupling, or a gradual recoupling as in the long-term relaxation $\Delta\dot{\Omega}_c(t) \sim t$.] We can therefore set $t_0 = \Delta\Omega_c/|\dot{\Omega}| \sim 10^d$. Since $\tau = 32^d$, $t_0 < \tau$, and the nonlinear response terms in equation (11) formally reduce, to accuracy

TABLE 1

OBSERVED PARAMETERS OF THE GLITCHES AND THE PARAMETERS OF THE BEST FITS FOR THE INDIVIDUAL POSTGLITCH DATA SETS AND OF THE CONSISTENT FIT, IN WHICH THE SAME SET OF RELAXATION TIMES $\tau_1 = 10$ HR, $\tau_2 = 3^d.2$ AND $\tau_3 = 32^d.7$ ARE ADOPTED FOR ALL THE POSTGLITCH DATA SETS

	GLITCH DATE							
PARAMETER	1969 Feb 28	1971 Aug 29	1975 Sep 9	1978 Jul 13	1981 Oct 10	1982 Aug 10	1985 Jul 12	1988 Dec 24
$[\Delta\Omega_c(0)/\Omega_c]_{-6}$	2.35	2.05	1.99	3.06	1.14	2.05	1.3	1.81
$[\Delta\dot{\Omega}_c(0)/\dot{\Omega}_c]_{-2}$	1.3	1.8	1.1	1.8	0.9	2.0	1.5	16.
Best Fits								
$[\Delta\dot{\Omega}_c(0)/\dot{\Omega}_c]^{lt}_{-3}$	7.08	7.25	7.1	6.48	6.39	6.1	6.51	4.32
$[\Delta\ddot{\Omega}_c/\lvert\dot{\Omega}_c\rvert]_{-6}\,d^{-1}$	4.41	5.24	6.93	4.77	10.5	3.85	6.7	2.99
τ_1 (hr)	...	...	...	...	...	...	...	10
τ_2 (d)	3.4	3.4	3.0	3.3	3.4	3.0	3.4	3.5
τ_3 (d)	34.6	32.6	30.3	38.8	32.5	30.0	31.1	29.0
a_1 (10^{-13} rad s^{-2})	0	0	0	0	0	0	0	2.11
a_2 (10^{-13} rad s^{-2})	1.98	6.13	1.64	4.77	3.92	5.8	4.71	6.8
a_3 (10^{-13} rad s^{-2})	2.85	3.03	2.02	7.17	0.74	6.17	2.8	4.52
χ^2 (best)	3.61	2.02	1.91	3.59	2.05	1.44	2.87	5.59
Degrees of freedom	7	11	5	9	6	13	16	7
Consistent Fit with $\tau_1 = 10$ hr, $\tau_2 = 3^d.2$, $\tau_3 = 32^d.7$								
$[\Delta\dot{\Omega}_c(0)/\dot{\Omega}_c]^{lt}_{-3}$	7.08	7.23	7.19	6.58	6.28	6.0	6.49	4.65
$[\Delta\ddot{\Omega}_c/\lvert\dot{\Omega}_c\rvert]_{-6}\,d^{-1}$	4.36	5.26	6.94	4.8	10.2	4.04	6.68	3.27
a_1 (10^{-13} rad s^{-2})	0.001	0.0002	0.0	0.0004	0.48	0.26	0.89	2.11
a_2 (10^{-13} rad s^{-2})	1.91	5.94	1.57	4.88	3.76	5.89	4.64	6.90
a_3 (10^{-13} rad s^{-2})	2.9	3.2	2.18	6.99	0.91	6.05	2.91	4.31
χ^2 (constant)	4.89	2.48	3.67	7.31	2.15	3.02	4.29	7.21

NOTE.—$a_i = (I_i/I)\ \Delta\Omega_c(0)/\tau_i\ \exp\ -(\Delta/\tau_i)$ denotes the amplitude of the exponential relaxation $\exp\ -t/\tau_i$ in the fit to $\Delta\dot{\Omega}_c(t)$, given in units of 10^{-13} rad s^{-2}. $[\Delta\dot{\Omega}_c(0)/\dot{\Omega}_c]^{lt}$ denotes the part of the jump in spindown rate associated with the long-term recovery, that is the intercept at $t = 0$ of the long-term straight line fit $\Delta\dot{\Omega}_c \propto t$. $\Delta\ddot{\Omega}/|\dot{\Omega}|$ is the slope of the long-term recovery $\Delta\dot{\Omega}_c \propto t$, given in units of 10^{-16} rad s^{-2} d^{-1}. τ_1 (hr), τ_2 (d), τ_3 (d) are the best-fitting relaxation times for each postglitch data set for the consistent fit, the values of a_i, $\Delta\dot{\Omega}_c$ (0) (long term) and $\Delta\ddot{\Omega}_c/|\dot{\Omega}|$ are given. For a comparison with the best fit on each postglitch data set, the χ^2 (consistent) and χ^2 (best) should be compared at the given number of degrees of freedom. The consistent fit gives a reasonable χ^2 on all postglitch data sets with the same parameters τ_2, τ_3.

TABLE 2

OBSERVED AND DEDUCED PARAMETERS FOR EIGHT VELA PULSAR GLITCHES ACCORDING TO THE CONSISTENT FIT

	GLITCH DATE							
PARAMETER	1969 Feb 28	1971 Aug 29	1975 Sep 28	1978 Jul 3	1981 Oct 10	1982 Aug 10	1985 Jul 12	1988 Dec 24
$[\Delta\Omega_c(0)/\Omega_c]_{-6}$	2.35	2.05	1.99	3.06	1.14	2.05	1.30	1.81
$[\Delta\dot{\Omega}_c(0)/\dot{\Omega}_c]_{-2}$	1.3	1.8	1.1	1.8	0.90	2.0	1.5	16
$[\Delta\ddot{\Omega}_c/\lvert\Omega\rvert]_{-6}\,d^{-1}$	4.36	5.26	6.94	4.8	10.2	4.04	6.68	3.27
Δ_{max} (d)	7	14	5	23	0.81	0.98	3.2	0.00
Δ(d)	5	0.9	5.0	2.8	0.5	0.9	0.2	0.00
$(I_1/I)_{-3}$	0.59	0.59	0.59	0.59	0.59	0.59	0.59	0.59
$(I_2/I)_{-3}$	1.5	1.5	1.5	1.5	1.5	1.5	1.5	1.5
$(I_3/I)_{-3}$	5.8	6.4	5.1	10.0	3.2	12.1	9.0	9.5
$(I_A/I)_{-3}$	7.1	7.2	7.2	6.6	6.3	6.0	6.5	4.7
$(I_B/I)_{-3}$	8.4	8.8	12.4	15.2	12.2	8.4	7.9	8.2
$(I_p/I)_{-2}$	2.3	2.5	2.7	3.4	2.4	2.9	2.6	2.5
$(\delta\Omega/\Omega)_{-4}$	1.9	1.6	1.2	1.6	0.73	1.7	1.2	1.7
t_g (days)	1624	1375	1036	1371	616	1485	972	1422
t_{obs} (days)	912	1491	1009	1227	272	1067	1261	907

NOTE.—The first four rows give the observed parameters: the jumps in rotation rate and spindown rate; the slope $\Delta\ddot{\Omega}_c/|\dot{\Omega}_c|$ of the long-term recovery in spindown rate, and the uncertainty Δ_{max} in the time of each glitch. There are three exponentially relaxing components with relaxation times $\tau_1 = 10$ hr, $\tau_2 = 3^d.2$, and $\tau_3 = 32^d.7$ which yield good fits to all postglitch data sets. The moment of inertia fractions in these three components are (I_1/I), (I_2/I), (I_3/I). The amplitudes of these exponential relaxation terms in $\dot{\Omega}_c$ are directly obtained from the fits and have the form $a_i = (I_i/I)\ (\Delta\Omega_c(0)/\tau_i)\ \exp\ -(\Delta/\tau_i)$, where Δ is the time when the postglitch observations start, measured from the actual date of the glitch. Δ values can be chosen to allow the same values of I_1/I and I_2/I after each glitch. This is not possible for I_3/I. Best-fit values of Δ (days) are given in the fifth row. I_A/I and I_B/I are the fractional moments of inertia of the superfluid regions responsible for the glitches, and in the case of I_A/I also for the long-term recovery. I_p/I is the sum of the fractional moments of inertia $[(I_p/I) = (\sum_i (I_i/I) + I_A + I_B)]$; it provides a lower bound to the fractional moment of inertia of the neutron star crust. $\delta\Omega/\Omega$ is the fractional decrease in superfluid rotation rate at a glitch, and t_g the theoretically expected time to the next glitch. The last row gives the observed time to the next glitch.

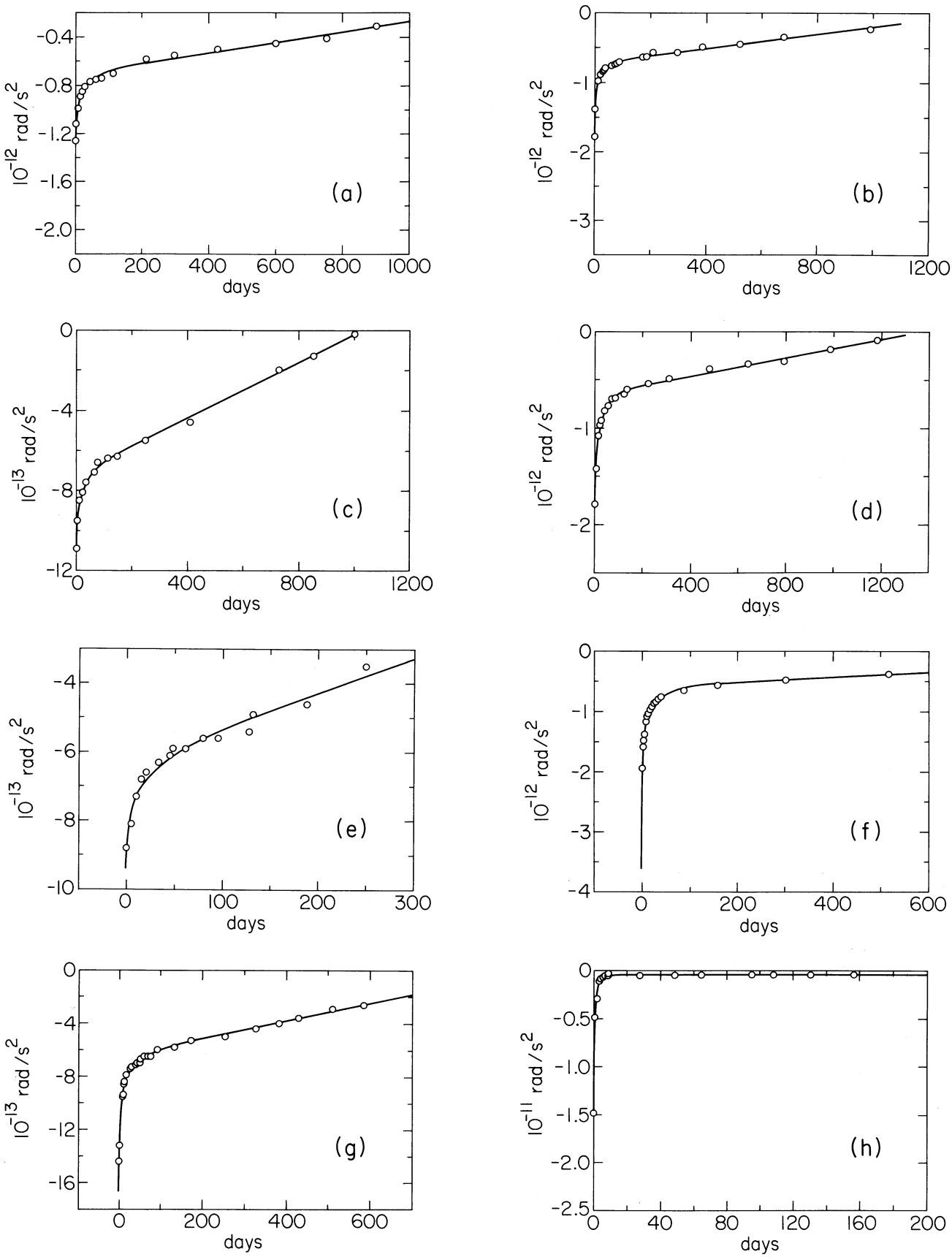

FIG. 4.—Observations of the spindown rate following each glitch, together with the consistent model fits, following each of glitches 1 to 8

t_0/τ, to a simple exponential of the same form as in the linear regime,

$$\lim_{t_0 \ll \tau} \Delta\dot{\Omega}_c(t)/\dot{\Omega}_{\text{nonlinear}} = (I_i/I)(t_0/\tau) \exp(-t/\tau) . \quad (14)$$

Thus, the observed 32^d exponential relaxation can reflect nonlinear response or linear response. It is not possible to test for these alternatives in the data as the accuracy of our multicomponent fit cannot distinguish a true nonlinear response for this component, or search for the higher order corrections to equation (14); using the full nonlinear response model yielded comparably good fits. We think it likely that the 32^d response is from a superweak pinning region in the nonlinear regime, but this is not a definite conclusion of the data analysis. As discussed in earlier work (Alpar et al. 1989), nonlinear relaxation times from weak pinning regions in the Vela pulsar are of the order of 1000^d. Therefore, if the 32^d response is to be nonlinear, it must come from a superweak pinning region.

The presence of a torque which varies linearly in time is a strong argument in favor of this assignment. Such a torque is a signature of a nonlinear regime; as we have noted earlier, it is understood as arising from the superposition of many small regions, k, in which $\delta\omega_k(0, r)$ varies linearly with r, provided their nonlinear relaxation times τ_n satisfy $\tau_n \lesssim t_0 \equiv \delta\Omega/|\dot{\Omega}|$, the maximum offset time of these nonlinear regions, through which vortices moved. Since τ_n in a weak pinning region is $\sim 1000^d$, this condition can be met only if the region in question is one of superweak pinning. Thus it is consistent to assume the 32^d relaxation is nonlinear. In this picture the same kinds of physical regions, involving superweak pinning and nonlinear response, are responsible for both the 32^d exponential relaxation *and* the long-term behavior $\Delta\dot{\Omega}_c \sim t$. Put another way, there are two separate contributions of this nonlinear response to postglitch behavior: (1) superweak pinning regions *through which vortices have not moved* give rise to a 32^d exponential relaxation; and (2) superweak pinning regions *through which vortices have moved* give rise to an internal torque which varies linearly in time. This situation arises naturally if the physical location of the vortex unpinning in a glitch resides within that part of the star in which the pinning is superweak and the response is nonlinear, as shown in Figure 2.

The weak-to-superweak pinning transition takes place at one specific density layer in the crust superfluid (Alpar et al. 1984b). According to the above reasoning, this critical density ρ^{sw} lies within the nonlinear response regions, so that it explains the 32^d relaxation time as a nonlinear relaxation time for the superweak regime. This assignment is only a consistent assumption. The transition density above which creep becomes linear is somewhat higher, $\rho^{tr} > \rho^{sw}$. A model calculation, shown in Figure 5, gives $\rho^{sw} = 8 \times 10^{13}$ g cm^{-3} and $\rho^{tr} = 8.6 \times 10^{13}$ g cm^{-3}. Associating the 32^d exponential relaxation and the nonlinear creep response $\Delta\dot{\Omega}_c(t) \propto t$ with this density range means that the fractional moment of inertia $(I_3/I + (I_A/I \sim 10^{-2}$ must reside at $\rho^{sw} < \rho < \rho^{tr}$. The regions A_1 are responsible for storing excess vortex density and releasing this stored density δn at each glitch. For simplicity, we assume that the moment of inertia of these regions is large compared to the moment of inertia of the vortex repinning regions A_2, $I_A \cong I_{A_1} \gg I_{A_2}$. The unpinned vortices then scatter outward, through the regions B. The moment of inertia I_B must therefore reside at densities $\rho < \rho^{sw}$, in nonlinear creep regions with weak pinning. The density ρ^{sw} must be (and is, in our model calculation) large enough that $I_B/I \sim 10^{-2}$, the largest moment of inertia in our fits. This constraint, that the extent of the crustal superfluid with $\rho < \rho^{sw}$ be large enough to have an

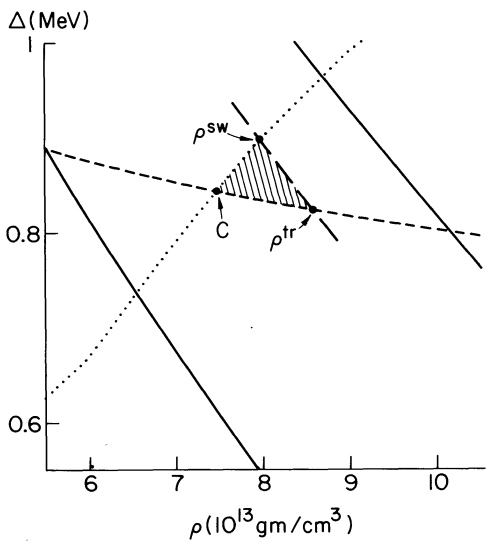

FIG. 5a

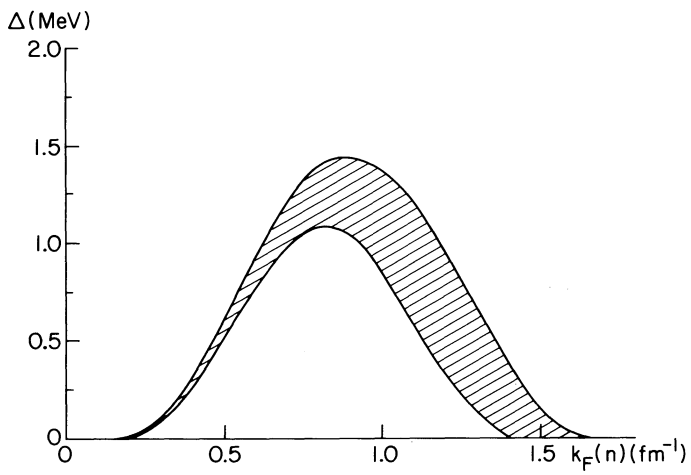

FIG. 5b

FIG. 5.—Some possible constraints on $\Delta(\rho)$ obtained from our identification of the presence of regions of superweak pinning in the nonlinear creep regime. The criteria for the transition from superweak to weak pinning (with $\gamma' = 1$) and for the transition from nonlinear to linear creep (with $\gamma = 0.5$) are plotted in the $\Delta - \rho$ plane, together with a band of gap functions, $\Delta(\rho)$, calculated by Ainsworth, Pines, & Wambach (1989), delineated by the bold curves, and shown below as Fig. 4*b*. We model this family of $\Delta(\rho)$ curves as $\Delta(\text{MeV}) = \Delta_0 - 2.63\ k_F\ (\text{fm}^{-1})$, with 3.5 MeV $< \Delta_0 <$ 4 MeV, in the density range displayed. For the above choice of γ and γ', $\Delta(\rho)$ curves which are above the point C and which pass through the shaded triangle are the only curves which are compatible with superweak pinning in the nonlinear creep regime. For these curves, ρ^{sw} and ρ^{tr} obtained from the intersection of $\Delta(\rho)$ with the critical lines for superweak to weak pinning and nonlinear to linear creep transitions satisfy $\rho^{sw} < \rho^{tr}$. This selection is illustrated for a particular $\Delta(\rho)$ curve, traced in long dashes, corresponding to $\Delta_0 = 3.73$ (MeV). This curve was also used to calculate the relaxation time displayed in Fig. 1. (*b*) The gap Δ(MeV) as a function of $k_F(\text{fm}^{-1})$, taken from Ainsworth, Pines & Wambach (1989). The density range of interest, studied in Fig. 5*a*, is the range of higher density where Δ decreases with ρ. (The relation between ρ and k_F is $\rho(10^{13}\ \text{g cm}^{-3}) = 5.64\,[k_F(\text{fm}^{-1})]^3$.)

inertial moment $\gtrsim 10^{-2}$, is satisfied for most neutron star models. A second consequence of our identification of the nonlinear time scale $\tau_n = 32^d$ is a determination of the effective distance, b, between superweak pinning sites. With equations (3) and (9), we find $b \cong 2500$ fm $\sim 80\ b_z$ for the superweak regime.

Having interpreted the 32^d time scale with superweak pinning in the nonlinear creep regime, at $\rho^{sw} < \rho < \rho^{tr}$, the $3^d.2$ exponential relaxation time scale is naturally interpreted as a time scale representing *linear* creep regions (with superweak pinning) at densities $\rho > \rho^{tr}$. As the linear creep relaxation time t_l depends sensitively on E_p, the presence of one (or a few) time scales in linear creep response must reflect a typical scale of pinning energies E_p in the superweak regime. At the transition to the linear creep regime at density ρ^{tr}, $\tau_n = \tau_l$ and $E_p = (E_p/kT)_{tr}\, kT = 0.34$ MeV, using equation (10) at the temperature $kT = 11$ keV. *If* we assume the relatively slowly varying nonlinear relaxation time τ_n has roughly the same value at ρ^{tr} as at ρ^{sw}, $\tau_l = \tau_n \sim 32^d$, then the $3^d.2$ linear creep relaxation time implies

$$E_p(3.2d) \cong E_p(32d) - kT \ln\left(\frac{32d}{3.2d}\right) \cong 0.32 \text{ MeV} \qquad (15)$$

using equation (7) for τ_l. The remaining, 10 hr, time scale reflects the regions with minimum pinning in the superweak linear creep regime and corresponds to the shortest time scales that could be resolved observationally. This time scale implies

$$E_p(10 \text{ hr}) \cong E_p(32^d) - kT \ln\left(\frac{32^d}{10 \text{ hr}}\right) \cong 0.29 \text{ MeV} . \qquad (16)$$

These estimates are based on the assumption that the variation in the observed linear creep relaxation times reflect small variations in E_p, rather than changes in the effective pinning distance b. As $\tau_l \propto b^{-1} \exp E_p/kT$, the latter possibility, which we consider unlikely, would require b to increase by a factor of $32^d/10$ hr $\simeq 80$, to $b \sim 6500\ b_z$, within the linear creep regions, a factor comparable to the increase in effective b at the weak to superweak pinning transition.

The pinning energies we infer are similar to plausible values for the weak pinning regime. Pinning energies for individual nuclei are not expected to be very different in the superweak pinning regime. To put this another way, a transition that substantially rescales the pinning energies would give a much larger factor between the linear creep relaxation times. For the Vela pulsar, equation (7) shows that at $kT = 11$ keV a jump by only 75 keV in E_p leads to a change in the relaxation times by a factor of a thousand, rendering it impossible to diagnose such a transition from a pair of relaxation times in the observable range.

The interpretation that the 32^d relaxation time reflects the presence of superweak pinning in the nonlinear regime places several constraints on models for the pinned crust superfluid:

1. The weak to superweak transition should fall within the nonlinear creep regime, that is, the critical density ρ^{sw} for this transition should be less than the critical density ρ^{tr} above which linear creep prevails (see Figs. 1 and 2).

2. The nonlinear relaxation time for superweak pinning ($\rho \gtrsim \rho^{sw}$) is 32^d.

3. The densities ρ^{sw} and ρ^{tr} should not be very different so that (as our fits indicate) the moment of inertia associated with the 32^d linear relaxation, as well as the moment of inertia I_A, where $\tau \sim 32^d \ll t_0$ is needed, is a small fraction of the moment of inertia in the crust superfluid, while ρ^{tr} should be "large enough" that most of the crust superfluid moment of inertia is in the nonlinear regime, as we discuss in the next subsection. Whether these constraints can be satisfied depends in turn on the superfluid gap as a function of density, the pinning energy as a function of the gap, and the ratio of ξ to b_z, which determines the criterion for the transition from weak to superweak pinning.

Since none of these quantities is known to, say, 20% accuracy, we parameterize all three in order to get an idea of the range of parameters which are consistent with the above constraints. We take as a representative superfluid energy gap the recent calculations of Ainsworth et al. (1989). They find a family of possible gap functions, whose behavior at densities of $7\text{–}12 \times 10^{13}$ g cm^{-3} may be parameterized as

$$\Delta(\text{MeV}) = -2.63 k_F(\text{fm}^{-1}) + \Delta_0(\text{MeV}) , \qquad (17)$$

where Δ_0 varies between 3.5 and 4. We parameterize the pinning energies, given in equation (2), as

$$E_p = \gamma \frac{3}{8\pi} \frac{\Delta^2 n}{E_F} V , \qquad (18)$$

where $\gamma \lesssim 1$. (An early calculation [Alpar et al. 1984b] yielded $\gamma \sim 0.1\text{–}0.6$ at the relevant densities.) Next, the uncertainty in the criterion for superweak pinning may be parameterized as

$$\xi_{sw} \geq \gamma'(b_z/2) , \qquad (19)$$

where $\gamma' > 1$. This condition can be written as

$$\Delta_{sw}(\text{MeV}) \leq \frac{26 k_F(\text{fm}^{-1})}{\gamma' b_z(\text{fm})} . \qquad (20)$$

Using equations (18) and (10) with $kT = 11$ keV, we find that at the linear-nonlinear creep transition,

$$\Delta_{tr}(\text{MeV}) = \frac{0.625}{\gamma^{1/2} k_F(\text{fm}^{-1})^{1/2}} . \qquad (21)$$

We show in Figure 5 the critical curves for the superweak-weak pinning and nonlinear-linear creep transition in the Δ-ρ plane (eqs. [20] and [21]), for $\gamma' = 1$ and $\gamma = 0.5$, together with the family of actual $\Delta(\rho)$ curves calculated by Ainsworth et al. (1989).

A set of mutual constraints relating γ, γ' and the gap function $\Delta(\rho)$ follow from our interpretation of the Vela pulsar data as requiring that $\rho^{sw} < \rho^{tr}$. Requiring that equation (20) be satisfied at a lower density than equation (21) brings in a consistency check for the gap result, equation (17). We find that for a range of parameters, the gap results given in equation (17) give consistent solutions. For given γ and γ', the intersection of the two critical curves, equations (20) and (21) defines a critical point C in the $\Delta - \rho$ plane, shown for $\gamma = 0.5$ and $\gamma' = 1$ in Figure 5. The location of this point C in relation to a given family of gap function curves $\Delta(\rho)$ determines whether $\rho^{sw} < \rho^{tr}$ is possible with those $\Delta(\rho)$. If C is below the range of $\Delta(\rho)$ curves, then all $\Delta(\rho)$ will allow $\rho^{sw} < \rho^{tr}$. If C is above the range of $\Delta(\rho)$, there is no gap model within that family of $\Delta(\rho)$ that will accommodate $\rho^{sw} < \rho^{tr}$. If C falls within the range of $\Delta(\rho)$, then only those gap curves $\Delta(\rho)$ above C lead to $\rho^{sw} < \rho^{tr}$. Using the parameterization of equation (17) to characterize the gap curves $\Delta(\rho)$, and taking the lattice spacing $b_z = 40$ fm, we

find that $\rho^{sw} < \rho^{tr}$ requires

$$\gamma^{1/3} > \left(\frac{0.63}{(\gamma')^{1/3}} + 2.55(\gamma')^{2/3}\right)\frac{1}{\Delta_0(\max)}, \quad (22)$$

where $\Delta_0(\max) = 4$ MeV for the family of $\Delta(\rho)$ curves calculated by Ainsworth et al. (1989). Thus, consistency with the APW results requires $\gamma > 0.5$ with $\gamma' = 1$, while taking $\gamma \leq 1$, for the definition of γ to be meaningful (see eqs. [2] and [18]) means that $\gamma' \leq 1.6$, which in turn means the transition to superweak pinning takes place when the coherence length is not more than $0.8b_z$. Applying restrictions on the allowed range of γ and γ' in turn introduces constraints on $\Delta(\rho)$ curves that allow $\rho^{sw} < \rho^{tr}$. The definite requirement $\gamma < 1$ means $\Delta_0(\max) \gtrsim 3.2$ MeV; so that a gap function peaking at $k_F \sim 0.8$ fm^{-1} must have a peak value of at least about 1 MeV, ruling out gaps $\Delta(\rho)$ that are significantly lower than the APW values. Gap functions that are much larger than the range calculated by Ainsworth et al. (1989) would be required only if one had an independent argument that γ' is relatively large; for example $\gamma' > 2$ would require a peak gap value of at least 2.4 MeV. It is rather striking that our interpretation of the Vela pulsar data with the requirement $\rho^{sw} < \rho^{tr}$ leads to a remarkable consistency with recent calculations of the gap functions $\Delta(\rho)$ and to constraints relating the pinning parameters γ and γ' to $\Delta(\rho)$ that yield plausible values for γ and γ' while arguing against very low gap values.

To summarize, consistent fits for the short time scale relaxation following the eight glitches of the Vela pulsar examined here require the linear response regime of the vortex creep theory, while the intermediate 32^d time scale exponential relaxation is interpreted as the response of a superweak pinning region that is in the nonlinear creep regime. All short and intermediate relaxation time scale ($\tau_1 = 10$ hr, $\tau_2 = 3^d.2$, $\tau_3 = 32^d$) lead to a range of acceptable pinning energies, which are consistent with estimates of pinning parameters based on current energy gap calculations (Ainsworth et al. 1989). The uncertainties in the latter are such that these calculations do not, at present, yield a unique set of parameters. Nevertheless, the present interpretation of the Vela data does require that the gap function $\Delta(\rho)$ must not be much weaker than the $\Delta(\rho)$ calculated by Ainsworth et al. (1989). Indeed, we can argue more generally that $\rho^{sw} \lesssim \rho^{tr}$, even if the 32^d response comes from the linear regime. The long time scale response $\Delta\dot{\Omega} \propto t$ must be in the nonlinear regime and with a relaxation time $\tau_A \ll t_g$, the time between glitches. Weak pinning relaxation times are long, $\tau_w \sim 1000^d \sim t_g$. Therefore the long time scale response indicates the presence of superweak pinning in the nonlinear regime. Now, if $\tau_3 = 32^d$ is associated with linear response, it cannot be very different from $\tau_A \ll 1000^d$ associated with the long time scale response in the nonlinear regime, so the corresponding pinning energies and therefore ρ^{tr} and ρ^{sw} must also be close to each other. Thus the above conclusions for the superfluid gap are likely to hold even if the 32^d response is not assumed to belong to the nonlinear regime.

4.2. *The Long-Term Behavior*

After the short and intermediate time scale exponential relaxation is completed, the remaining $\Delta\dot{\Omega}_c(t)$ settles to a slow recovery that is linear in t. This behavior is observed after each of the eight Vela pulsar glitches and persists until the arrival of the next glitch. The basic question here is whether the entire spin-up introduced by the glitch relaxes back in the course of this slow recovery, or whether a portion of the spin-up remains. In other words, does a glitch heal before the next one comes along? Does relaxation trigger the next glitch or do unrelaxed remnants of spin-up from each glitch form part of the long-term dynamics?

A glitch at time $t = 0$ will have completely relaxed at some later time t if the integrated negative offset in the spindown rate compensates exactly for the initial frequency increase:

$$\Delta\Omega_c(t) = \Delta\Omega_c(0) + \int_0^t \Delta\dot{\Omega}_c(t)dt = 0 . \quad (23)$$

Without integrating to test for this condition, one can examine the spindown rate directly to see if the relaxation process is completed, in which case the spindown rate will have a constant equilibrium value, apart from a small second derivative of the rotation rate due to the pulsar braking torque. In vortex creep theory this equilibrium would be reached when vortex creep has restarted in all perturbed nonlinear response regions. Completion of the relaxation towards equilibrium should involve an increase in the slope of $\Delta\dot{\Omega}_c(t)$ or even a steplike positive change, indicating the "Fermi-function" response of a large nonlinear creep region, as parts of the superfluid where previous vortex creep was stopped by the glitch restart to allow vortex creep and thereby recouple to the crust's $\dot{\Omega}_c$. A search for such signatures was emphasized as an indicator of the relation between the healing of one glitch and the occurrence of the next (Alpar et al. 1984).

No signs of change in the long-term postglitch relaxation with $\Delta\dot{\Omega}_c(t) \propto t$ were seen prior to the occurrence of the next glitch in a study of the first six glitches (Cordes et al. 1988). This was also the case for the seventh and eighth glitches. The question can be posed in model-independent fashion (Blandford 1990) by comparing the extrapolation with timing parameters prior to the first glitch, assuming no glitches have occurred, with the observed rotation frequency at a later epoch after several glitches have occurred. Making the comparisons between the extrapolated rotation rate and the observed value just before the sixth glitch, one finds that the first five glitches leave a collective remnant spin-up of a part in 10^5, after their observed (partial) relaxation. This remnant spin-up is indeed a significant portion of the sum of the initial frequency increases from these glitches. Thus the glitches contribute a net spin-up to the crust against the dominating background of spindown by the external torque and have the same spin-up signature as the continuous internal torques of vortex creep (equation [5]). This means that the unrelaxed part of the glitches is simply a discrete complement to the continuous creep torque between the interior and the crust (Alpar 1992; Pines & Alpar 1992). The continuous outward creep of vortices is supplemented by occasional unpinnings of large numbers of vortices whose sudden outward motion is manifested as the glitches.

The single observed long time scale component of $\Delta\dot{\Omega}_c(t)$ between glitches persists with a linear dependence on t until the next glitch. We interpret this term as a gradual recoupling of regions of nonlinear creep whose initial offset (decrease in superfluid rotation rate) at the last glitch, $\delta\Omega(r)$, translates into a succession of recoupling times $t_0(r) = \delta\Omega(r)/|\dot{\Omega}|$ and an increase in the recoupled superfluid moment of inertia. To the extent that $\delta\Omega(r)$ increases linearly with r in these regions, this increase is linear in time until the total moment of inertia I_A has recoupled at a time t_g. The maximum offset defines the time scale $t_g = \delta\Omega/|\dot{\Omega}|$ (also labeled t_B or t_0 in previous work) which

characterizes the time to the next glitch as we demonstrate below. In this model (Alpar et al. 1984b) the observed slope $\Delta\ddot{\Omega}$ of this term is

$$\frac{\Delta\ddot{\Omega}}{|\dot{\Omega}|} = \frac{I_A}{It_g} . \tag{24}$$

The contribution of vortex motion through the regions A at a glitch to angular momentum balance is $\frac{1}{2}I_A\,\delta\Omega$, since the average $\delta\Omega(r)$ is $\delta\Omega/2$. In addition, there will be regions whose moment of inertia we have denoted by I_B, through which a large number N of vortices move at a glitch, leading to a constant $\delta\Omega$ in these regions; this behavior is to be contrasted with that of the regions A, where the density of vortices that move at a glitch is constant while their total number and hence the associated $\delta\Omega(r)$ is incremental, until reaching the maximum $\delta\Omega$ in the adjacent regions B as depicted in Figure 2 (Alpar et al. 1984b; Cheng et al. 1988). Adding the contributions of regions A and B, the angular momentum balance in equation (12) is obtained.

We need a third equation to solve for I_A/I, I_B/I and $\delta\Omega$ in each postglitch fit. This is the equation describing the effect of the glitch-associated vortex motion through regions A and B on the crustal spindown rate $\Delta\dot{\Omega}$, since the vortex motion and the consequent $\delta\Omega(r)$ will stop vortex creep and result in a $\Delta\dot{\Omega}_c$. Since the regions A are observed to be recoupling, we postulate that they must have been stopped from creep immediately after a glitch, and thus contributed a term I_A/I to the initial offset $\Delta\dot{\Omega}_c/\dot{\Omega}$ of the crust's spindown rate. Figure 3*a* shows the contributions of our model regions A to $\Delta\dot{\Omega}_c$ at, and after, a glitch.

An ambiguity arises as to the extent of the regions B that were creep regions decoupled by the glitch, waiting to recouple at the offset time t_g. Formally, the question is what combination of I_B/I and I_A/I is responsible for the observed $\Delta\dot{\Omega}_c$. In previous work (Alpar et al. 1984b; Pines 1991) regions B were assumed to be creep regions decoupled by the glitch and therefore contributing fully to the initial $\Delta\dot{\Omega}_c/\dot{\Omega}_c$. If this were the case, the contributions of regions B to $\dot{\Omega}_c$ at and after a glitch would be as shown in Figure 3*b*. As we discussed above, this is not the case, for two reasons. First, we never observe any signs of sudden recoupling around a time t_g after the glitch; second, we do not see the integrated effect of a constant negative $\Delta\dot{\Omega}_c$ due to such regions B, which, if operative for a time t_g after each glitch, should cancel the spin-up contribution due to vortex motion through B, so that there would be no remnant spin-up contributions from the glitches. Thus, from the observations, we conclude *that the regions B contribute to the angular momentum transfer at the time of the glitch*, because unpinned vortices rapidly move through these regions, but they do not have the signature depicted in Figure 3*b* that would be expected if they were temporarily decoupled creep regions. We identify regions B as regions that cannot sustain a local vortex density and vortex current; they do not decouple from creep, because they never sustained vortex creep before or after a glitch; their only mode of coupling to the crust is by the discrete angular momentum transfer through sudden vortex motion at the glitches. We had already noted the presence of such regions and their role in glitches in earlier work (Cheng et al. 1988). With this identification, we arrive at a very simple form for our equation of the glitch-induced change in $\dot{\Omega}_c$:

$$\left(\frac{\Delta\dot{\Omega}_c}{\dot{\Omega}_c}\right)^{lt} = \frac{I_A}{I} \tag{25}$$

where the superscript, "*lt*," indicates that the contributions of the short and intermediate time scale linear response discussed in the previous subsection have been subtracted from $\Delta\dot{\Omega}_c/\dot{\Omega}_c$. A first report of this interpretation of the Vela pulsar's dynamics was given by Pines & Alpar (1992).

The values of I_A/I, I_B/I, $(\delta\Omega/\Omega)$, and t_g obtained by solving equations (12), (24), and (25) are given in Table 1 for each of the eight glitches. It is remarkable that, in addition to the consistent ranges of these parameters after independent fits to the separate sets of postglitch data, the calculated times t_g are on the average close to the observed times to the next glitch. A large discrepancy, by a factor ~ 2, is observed only after glitches 1 and 5. The total of t_g calculated for the first eight glitches agrees remarkably well with the sum of the observed interglitch time intervals; thus we find

$$\sum_{i=1}^{8} t_g^i = 9901^{\mathrm{d}} \tag{26a}$$

$$\sum_{i=1}^{8} t_{\mathrm{obs}}^i = 8146^{\mathrm{d}} . \tag{26b}$$

The discrepancy between these sums is 21%, while the rms deviation of the t_{obs}^i from their mean is 33% of the mean. The discrepancy between t_g^i and t_{obs}^i probably reflects the fluctuations in the number of vortices that unpin at each glitch. As the total number of glitches M increases, we would expect the fractional discrepancy between the *average* t_g and t_{obs} over a sample of M glitches to decrease as $(M/M)^{1/2}$. Note that on the average the glitch regions B spin down at the rate $\langle\delta\Omega/t_{\mathrm{obs}}\rangle$ and this is simply $\langle\delta\Omega/t_g\rangle = |\dot{\Omega}|$ in the long run, as $\langle t_{\mathrm{obs}}\rangle \to \langle t_g\rangle$; i.e., in the long run the glitches permit the regions B to spin down at the same rate as the rest of the star. *The glitches are simply the discrete events coupling those regions of the crustal superfluid that physically cannot sustain continuous vortex creep.* The mechanism that triggers these discrete events is still not known.

5. CONCLUSIONS

We have evaluated eight of the nine glitches and postglitch relaxation observed for the Vela pulsar to date with a comprehensive model involving the vortex dynamics of the pinned superfluid in the neutron star crust. Independent fits to each set of postglitch data produced sets of parameters for the crust superfluid which are both plausible in the light of theoretical estimates and remarkably consistent for all the postglitch data sets.

There is some uncertainty in our estimate of the moment of inertia (I_3/I), which is associated with an uncertainty in our interpretation of the 32^{d} relaxation time. The model we have proposed associates the 32^{d} relaxation with a region of superweak pinning and nonlinear response, region 3, where no vortex motion takes place at a glitch. This means $I_3/I = a_3\,\tau/\Delta\Omega_c$. A much smaller value of $I_3/I = a_3\,\tau/\overline{\delta\Omega}$ is obtained if the 32^{d} relaxation time is alternatively associated with a region through which vortices move at the time of a glitch (such a region is necessarily a region of linear response). Here $\overline{\delta\Omega}$ is the mean decrease in superfluid rotation rate in region 3 produced by vortex motion through this region. In this case $\overline{\delta\Omega}$ is of the order of $\delta\Omega$ and can be obtained by using equation (12), modified to include the angular momentum transfer $I_3\,\overline{\delta\Omega}$, together with equations (2.4) and (2.5). The values of (I_3/I) and (I_p/I) which result from this alternative interpretation are given in Table 3.

TABLE 3

DEDUCED PARAMETERS FOR EIGHT VELA GLITCHES BASED ON THE INTERPRETATION THAT VORTICES PASS THROUGH REGION (3) AT THE TIME OF THE GLITCH

	GLITCH DATA							
PARAMETER	1969 Feb 28	1971 Aug 29	1975 Sep 28	1978 Jul 3	1981 Oct 10	1982 Aug 10	1985 Jul 12	1988 Dec 24
$(I_3/I)_{-3}$	0.14	0.16	0.16	0.37	0.10	0.28	0.20	0.20
$(I_p/I)_{-2}$	1.77	1.71	2.17	2.41	2.06	1.67	1.65	1.51

NOTE.—We list only the values of the two parameters affected by this alternative interpretation, (I_3/I) and $(I_p I)$.

In terms of neutron star structure, our fits yield the important constraint that *the moment of inertia in the crust superfluid is at least* 2.4% *of the star's total moment of inertia.* To get neutron star models with a thick enough crust to satisfy this constraint requires a neutron matter equation of state that is at least "moderately stiff" (Pandharipande et al. 1976; Pines 1991; Datta & Alpar 1993).

Our fits show that postglitch response in the Vela pulsar comes in two categories. The short time scale response ($\tau = 0^d.4$, $3^d.2$, represents the prompt response of regions of the superfluid through which no vortices move at the time of a glitch. These regions respond only to the increase in the crust rotation rate, i.e., to the observed glitches. As noted above, the $3^d.2$ response may also be of this kind, or alternatively, may be associated, in part, or entirely, with a region through which vortices move at the time of the glitch.

It is in the long-term response that we see the interplay between glitches and postglitch response. The long-term response in Vela comes from nonlinear creep regions that are affected by sudden vortex motion at the time of the glitch. From an analysis of the postglitch data to date, it seems clear that an initial decrease in $\dot{\Omega}_c$ followed by a recovery that is linear in time, $\Delta\dot{\Omega}_c(t) = \Delta\dot{\Omega}_c(0)\,[1 - (t/t_g)]$ is the only long-term signature of interglitch $\dot{\Omega}_c$, once the prompt postglitch exponentials have relaxed. We ascribe this long-term recoupling to nonlinear vortex creep regions which act as vortex unpinning and repinning reservoirs and which supply the vortex unpinnings that are observed as glitches. The subsequent reduction in creep rate translates to a decrease in $\dot{\Omega}_c$ (an increase in the absolute value of the spindown rate) which gradually heals as vortices start to creep and refill these pinning regions. This interpretation of the long-term $\Delta\dot{\Omega}_c(t)$ was already invoked in our earlier work (Alpar et al. 1984b; Pines 1991). In the present work we have added to this general framework the interpretation that the regions through which vortices move macroscopically during a glitch (regions B), in distinction from the unpinning and repinning regions (regions A), can *never* sustain vortex creep at interglitch epochs. They therefore do not contribute to the sudden change in $\dot{\Omega}_c$ associated with the glitch. These vortex depletion regions, whose physical origin we had discussed earlier (Cheng et al. 1988), spin down only in discrete lumps of vortex transfer, at the time of the glitches, which are now seen as the discrete component of the spin-up internal torques coupling the crustal superfluid to the crust. The major part of the spin-up at glitches is simply the long-term coupling of these vortex depletion regions to the overall spindown of the star under the external torque; it therefore does not relax back. We thus see the glitches and interglitch creep as two components of the same process of vortex motion coupling the crustal superfluid to the crust. The reason for the particular size of glitches (or number of vortices unpinning at each glitch) for the Vela pulsar is a subject to be taken up in subsequent work, along with the evolution of glitch activity and the size distribution of glitches as a function of pulsar age.

We expect the behavior discussed here to be seen in the data following glitch 9, and after future glitches. Most of the initial $\Delta\dot{\Omega}$ of glitch 9 should decay exponentially with a time scale τ_1 of about 10 hr, possibly shorter, depending on the resolution of the earliest timing data, as this time scale, observed only after glitch 8 previously, is likely to be the minimum observationally resolvable relaxation time of linear creep with superweak pinning. We expect exponential relaxations $\tau_2 = 3^d.2$ and $\tau_3 = 32^d$ with I_2/I and I_3/I similar to the values found in this work. These components of postglitch relaxation should be followed by a long-term response $\Delta\dot{\Omega}_c(t) \propto t$. The I_A/I and I_B/I extracted from an analysis of glitch 9 should likewise give values in the range found for the previous eight glitches, $I_A/I \sim 10^{-2}$ and $I_B/I \sim 10^{-2}$, yielding a total $I_p/I \lesssim 3 \times 10^{-2}$. Finally, we expect the agreement between the average estimated and observed times from one glitch to the next to persist.

This work was partially supported by a NATO Collaborative Research grant 900074, by NSF grants INT89-18665 and NSF PHY86-00377, and by the Scientific and Technical Research Council of Turkey, grant TBAG1049. We thank Roger Blandford for stimulating discussions, the referee for a number of useful suggestions, and the Aspen Center for Physics for hospitality during several stages of this collaboration.

REFERENCES

Ainsworth, T. L., Pines, D. & Wambach, J. 1989, Phys. Lett. B, 222, 173
Alpar, M. A., 1977, Ph.D. thesis, Cambridge Univ.
———. 1992, in Structure and Evolution of Neutron Stars, ed. D. Pines, R. Tamagaki, & S. Tsuruta (Reading, MA: Addison-Wesley), 148
Alpar, M. A., Anderson, P. W., Pines, D., & Shaham, J. 1984a, ApJ, 276, 325
———. 1984b, ApJ, 278, 791
Alpar, M. A., Brinkmann, W., Kiziloğlu, Ü., Ögelman, H., & Pines, D. 1987, A&A, 177, 101
Alpar, M. A., Cheng, K. S., & Pines, D. 1989, ApJ, 346, 823
Alpar, M. A., Cheng, K. S., Pines, D., & Shaham, J. 1988, MNRAS, 233, 25
Alpar, M. A., Langer, S. A., & Sauls, J. A. 1984c, ApJ, 282, 533
Alpar, M. A., Nandkumar, R., & Pines, D. 1985, ApJ, 288, 191
Alpar, M. A., & Sauls, J. A. 1988, ApJ, 327, 723
Anderson, P. W., Alpar, M. A., Pines, D., & Shaham, J. 1982, Phil. Mag. A, 45, 227
Anderson, P. W., & Itoh, N. 1975, Nature, 256, 25
Baym, G., Epstein, R. I., & Link, B. 1992, Physica B, 178, 1
Bildsten, L., & Epstein, R. I. 1989, ApJ, 342, 951
Blandford, R. 1990, unpublished remarks at the US–Japan Seminar on the Structure and Evolution of Neutron Stars
Chau, H. F., & Cheng, K. S. 1991, Phys. Rev. A, 44, 3478
Cheng, K. S. 1987a, ApJ, 321, 779
———. 1987b, ApJ, 321, 805
Cheng, K. S., Alpar, M. A., Pines, D., & Shaham, J. 1988, ApJ, 330, 835
Cordes, J. M., Downs, G. S., & Krause-Polstorff, J. 1988, ApJ, 330, 841
Datta, B., & Alpar, M. A. 1993, in preparation

Epstein, R. I., & Baym, G. 1988, ApJ, 328, 680
———. 1992, ApJ, 387, 276
Flanagan, C. S. 1989, IAU Circ., No. 4695
———. 1990a, Nature, 345, 416
———. 1990b, private communication
———. 1991, IAU Circ., No. 5311
Gudmundsson, E., Pethick, C. J., & Epstein, R. I. 1982, ApJ, 259, L19
Hamilton, P. A., King, E. A., McConnell, D., & McCulloch, P. M. 1989, IAU Circ., No. 4708
Hamilton, P. A., McCulloch, P. M., & Royle, G. W. R. 1982, IAU Circ., No. 3729
Henis, Z., & Shaham, J. 1981, unpublished
Jones, P. B. 1990a, MNRAS, 243, 257
———. 1990b, MNRAS, 244, 675
———. 1990c, MNRAS, 246, 315
———. 1991, ApJ, 373, 208
———. 1992, Oxford University preprint
Klekociuk, A. R., Flanagan, C., McCulloch, P. M., & Hamilton, P. A. 1985a, in AIP Conf. Proc. (Adelaide)
Klekociuk, A. R., McCulloch, P. M., & Hamilton, P. A. 1985b, IAU Circ., No. 4089
Lyne, A. G. 1991, private communication
Lyne, A. G., & Pritchard, R. S. 1987, MNRAS, 229, 223
McCulloch, P. M., Hamilton, P. A., McConnell, D., & King, F. A. 1990, Nature, 346, 822
McCulloch, P. M., Hamilton, P. A., Royle, G. W. R., & Manchester, R. N. 1981, IAU Circ., No. 3644
———. 1983, Nature, 302, 319
McKenna, J., & Lyne, A. G. 1990, Nature, 343, 349
Ögelman, H., & Zimmermann, H. U. 1989, A&A, 214, 179
Pandharipande, V. R., Pines, D., & Smith, R. A. 1976, ApJ, 208, 550
Pines, D. 1971, in Proc. of 12th Intl. Conf. on Low Temperature Physics, ed. E. Kanda (Tokyo: Academic Press of Japan)
———. 1991, in Neutron Stars: Theory and Observation, ed. D. Pines & J. Ventura (Dordrecht: Kluwer), 57
———. 1992, in Structure and Evolution of Neutron Stars, ed. D. Pines, R. Tamagaki, & S. Tsuruta (Reading, MA: Addison-Wesley), 7
Press, W. H., Flannery, B. P., Teukolsky, S. A., & Vetterling, W. A. 1986, Numerical Recipes: The Art of Scientific Computing (Cambridge: Cambridge Univ. Press)
Radhakrishnan, V., & Manchester, R. N. 1969, Nature, 222, 228
Reichley, P. E., & Downs, G. S. 1969, Nature, 222, 551

Note added in proof.—Timing data for the first 200 days following the ninth glitch have now been analyzed by H. F. Chau, P. M. McCulloch, R. Nandkumar, & D. Pines (private communication [1993]), who find excellent agreement between the observations and the above predictions.